Electronic Supplementary Material (ESI) for Nanoscale.
This journal is © The Royal Society of Chemistry 2019

Self-assemblied CeVO4/Ag Nanohybrid as Photoconversion Agents with Enhanced Solar-driven Photocatalysis and NIR-responsive Photothermal/Photodynamic Synergistic Therapy Performance

Mengyu Chang,[ab] Meifang Wang,[ab] Yeqing Chen,[d] Mengmeng Shu,[e] Yajie Zhao,[ab] Binbin Ding,[ab] Zhiyao Hou,*[ac] and Jun Lin*[ab]

[a.] *State Key Laboratory of Rare Earth Resource Utilization, Changchun Institute of Applied Chemistry, Chinese Academy of Sciences, Changchun 130022, Jilin (China)*

[b.] *University of Science and Technology of China, Hefei, Anhui, 230026, China.*

[c.] *Laboratory of Protein Modification and Degradation, School of Basic Medical Sciences, Guangzhou Medical University, Guangzhou 511436, P. R. China*

[d.] *School of Applied Physics and Materials, Wuyi University, Jiangmen 529020, P. R. China*

[e.] *Department of Periodontology, Stomatological Hospital, Jilin University, Changchun 130021, P. R. China*

Experimental Section

Materials and Reagents: All of the chemicals used were of analytical grade and were used without further purification. Sodium hydroxide (NaOH), ammonium metavanadate (NH_4VO_3), silver nitrate ($AgNO_3$), fluorescein isothiocyanate (FITC) were purchased from Aladdin. Oleic acid (OA), $Ce(NO_3)_3 \cdot 6H_2O$, $Nd(NO)_3$ were purchased from Science and Technology Parent Company of Changchun Institute of Applied Chemistry. Tetrahydrofuran (THF), n-butanol, cyclohexane were purchased from Beijing chemical works. 2,2-Dimethoxy-2-phenylacetophenone (DMPA) was purchased from Tokyo Chemical Industry. Thiol-polyethylene glycol with different chemical groups ($HS\text{-}PEG_{1000}\text{-}OH$, $HS\text{-}PEG_{1000}\text{-}NH_2$) were purchased from PegBio Co., Ltd (Jilin, China).

Characterization: The X-ray diffraction (XRD) patterns were tested with a D8 Focus diffractometer (Bruker) with the use of Cu Kα radiation (λ = 0.15405 nm). Transmission electron microscopy (TEM) was recorded using a FEI Tecnai G2 S-Twin with a field emission gun operating at 200 kV. Fouriertransform Infrared spectra (FT-IR) were measured on a Vertex Perkin–Elmer 580BIR spectrophotometer (Bruker) with the KBr pellet technique. The UV-Vis adsorption spectral values were measured on a U-3310 spectrophotometer (Hitachi). The X-ray photoelectron spectra (XPS) were taken on a VG ESCALAB MK II electron spectrometer using Mg Kα (1200 eV) as the excitation source. Dynamic light scattering (DLS) and Zeta potential were obtained by using a Malvern instrument Zetasizer Nano system. Thermogravimetric analysis (TGA) of the products were performed using a Setaram TGA 92 instrument in the temperature range from room temperature to 800 °C at a heating rate of 10 °C min^{-1} in nitrogen. The UV-vis diffuse reflectance spectra were obtained from Lambda 35 spectrophotometer (PerkinElmer). Inductively Coupled Plasma (ICP) was taken on an iCAP 6300 of Thermo scientific. MSOT was taken inVision 128 small animal imaging system (iThera Medical

GmbH, Munich, Germany).

Statistical Analysis: Statistical analysis was performed with the Statistical Program for Social Sciences software (SPSS, Chicago, IL, USA) as needed. All data were expressed as means (standard deviation, and a statistically significant difference was considered to be present at $p < 0.05$. Except as mentioned, all assays were repeated in triplicate in three independent experiments.

Materials Synthesis:

1) Synthesis of Oleic Acid-Capped $CeVO_4$ Nanosheets:

$CeVO_4$ nanosheets were prepared according to the previous literature.[1] 0.6 g NaOH and 0.0585 g NH_4VO_3 were added to 5 mL water under magnetic stir. A mixed solution of 9 mL oleic acid and 10 mL ethanol was added under strong agitation. Then 1 mL $Ce(NO_3)_3 \cdot 6H_2O$ aqueous solution (1 M) was added dropwise. After stirring for 10 min, the mixture was transferred into a 40 mL Teflon-lined vessel, which was sealed in an autoclave and then treated for 8 hours at 140 °C. As the autoclave cooled to room temperature naturally, the samples could be collected from the bottom of the vessels by dissolving in cyclohexane. Finally, $CeVO_4$ nanosheets were centrifuged at 3000 rpm for 5 min, and washed three times with cyclohexane and ethanol. Then, the $CeVO_4$ nanosheets were dispersed in 5 ml cyclohexane.

2) Synthesis of HS-PEG-functionalized $CeVO_4$ Nanosheets:

Hydrophobic $CeVO_4$ nanosheets were converted into hydrophilic ones *via* a facile thiol-ene click method.[2] The 2 mL of above $CeVO_4$ nanosheets were precipitated by adding enough ethanol and collected by centrifugation at 3000 rpm for 5 min. Then the samples were dissolved into 2 mL of THF solution. Then 0.2 g of HS-PEG_{1000}-OH and 100 μL of photoinitiator DMPA (10 mg/mL) dissolved in THF were added. The mixture was irradiated with UV-light (1000 W, 365 nm wavelength) for 60 min in an

ice bath under magnetic stirring. After completion of UV irradiation, the HS-PEG-functionalized $CeVO_4$ nanosheets were collected by centrifugation at 12000 rpm for 15 min, and washed three times with deionized water.

2) Synthesis of $CeVO_4$/Ag Heterojunction Nanocrystals:

The $CeVO_4$/Ag heterojunction nanocrystals were one-step synthesized. Briefly, The above HS-PEG-functionalized $CeVO_4$ nanosheets dispersed in 5 mL n-butanol was added dropwise into $AgNO_3$ solution (0.01 M) dispersed in 5 mL n-butanol, then nitrogen gas was introduced to provide protective atmosphere. The mixture was refluxed at 90 °C for 4 h in the dark. The products were collected by centrifugation at 12000 rpm for 10 min and washed three times with deionized water.

3) Contrast Experiment:

In addition, for verifying the redox environment playing a decisive role in synthesizing $CeVO_4$/Ag, we implemented contrast experiment under same conditions except using $Nd(NO_3)_3$ instead of $Ce(NO_3)_3 \cdot 6H_2O$ to test whether $NdVO_4$/Ag could be synthesized.

Photocatalytic Degradation of Methyl Blue: In order to compare photocatalytic property of as-prepared $CeVO_4$/Ag with $CeVO_4$, we dispersed 15 mg materials into 3 mL methyl blue aqueous solution (50 mg/L). Before irradiation under the solar light, the mixture solution was stirred in darkness for 30 min to attain absorption-desorption equilibrium. After different time intervals of degradation under the solar light, the supernatant was collected and its absorption was measured using a UV-vis spectroscopy. Considering the factors of methyl blue self-degradation under the solar light, the absorption of methyl blue was measured under the same condition.

Extracellular $\cdot O_2^-$ Detection. For the extracellular $\cdot O_2^-$ generation test, a 1, 3-diphenylisobenzofuran (DPBF) probe was employed to detect the ROS. 10 μL of DPBF (10 mg/mL) solution was added to 3 mL of $NdVO_4$ or $NdVO_4$/Au (5 mg/mL) aqueous solution. Then the mixtures were irradiated under 808 nm

laser (1.0 W/cm^2) for different times (0, 5, 10, 20, 30 and 60 min). Afterwards, the supernatant was collected and its absorption was measured by a UV-vis spectroscopy.

Extracellular ·OH Detection. For the extracellular ·OH generation text, we dispersed 15 mg materials into 3 mL MB aqueous solution (50 mg/L). Before irradiation under the solar light, the mixture solution was stirred in darkness for 30 min to attain absorption-desorption equilibrium. After different time intervals (0, 5, 10, 20, 30 and 60 min) of degradation under the 808 nm (1.0 W/cm^2) irradiation, the supernatant was collected and its absorption was measured using a UV-vis spectroscopy.

Photothermal Effect of $CeVO_4$ and $CeVO_4$/Ag in Aqueous Solution: The aqueous $CeVO_4$ and $CeVO_4$/Ag solution (0.1 mL) was added into 96-well plates separately at different concentrations (0, 50, 100, 150 and 200 μg mL^{-1}) and was exposed to the NIR laser (808 nm, 1.9 W/cm^2) for 5 min. Simultaneously, an infrared camera (NEC, with an accuracy of 0.1 °C) was used to measure the real-time temperature, and the change in temperature was recorded every 15 s. And, the photothermal effect of aqueous $CeVO_4$ and $CeVO_4$/Ag solution with the same concentration of 200 μg mL^{-1} and different power density (0.7, 1.0, 1.3, 1.6 and 1.9 W/cm^2) was also measured in the same way.

Photothermal Conversion Efficiency of $CeVO_4$ and $CeVO_4$/Ag in Aqueous Solution: To examine the photothermal conversion efficiency, the aqueous solution of $CeVO_4$ and $CeVO_4$/Ag with concentration of 0.2 mg/mL (1 mL) was irradiated using an 808 nm laser (BWT Beijing Ltd., China) with power density of 1.3 W/cm^2 for 20 min, which was followed by natural cooling for another 20 min. Subsequently, 1 ml of deionized water was measured in the same way. The temperature was recorded using the infrared camera.

The photothermal conversion efficiency (η) of $CeVO_4$ and $CeVO_4$/Ag could be calculated

according to the the eq1

$$\eta = \frac{\mathrm{hS}(T_{\mathrm{max}} - T_{\mathrm{surr}}) - Q_{dis}}{I(1 - 10^{-A_{808}})} \quad (1)$$

The Tmax (K) means the equilibrium temperature; Tsurr (K) is ambient temperature of the surroundings. The Qdis (W) is heat loss from light absorbed by the container, and it was calculated to be approximately equal to 0 mW. I (W/cm^2) represents incident laser power density; A808 is the absorbance of samples at 808 nm. Where h (W/(cm^2·K)) means heat transfer coefficient, S (cm^2) represents the surface area of the container, the hS is calculated from the Figure 2F and S14B using the following eq 2

$$\tau_s = \frac{\mathrm{m}_D c_D}{hs} \quad (2)$$

Where τs is the sample system time constant, m_D and c_D are the mass (1 g) and heat capacity (4.2 J/(g·℃)) of the solvent. Thus, according to the calculation, the heat conversion efficiency (*η*) of the samples is listed in the table.

	Tmax-Tsurr	A808	τs	*η*
$CeVO_4$	9	0.265	779.54	14.91 %
$CeVO_4$/Ag	18	0.561	624.17	23.48 %

Ag ions release test. The $CeVO_4$/Ag (200 μg/mL) aqueous solution was irradiation with NIR laser (1.9 W/cm^2) for 10 min, then the supernatant were collected by centrifugation at 10000 rpm for 10 min. The Ag ions concentrations were measured by ICP-MS. Meanwhile, the supernatant of $CeVO_4$/Ag (200 μg/mL) aqueous solution without NIR laser irradiation was also detected as control.

Cell Culture: The HeLa cells line was cultured in DMEM culture medium supplemented with 1% (v/v)

penicillin, 1% (v/v) streptomycin, and 10% (v/v) fetal bovine serum at 37 °C in 5% CO_2. L929 cells line was cultured in MEM culture medium supplemented with 1% (v/v) penicillin, 1% (v/v) streptomycin, and 10% (v/v) fetal bovine serum at 37 °C in 5% CO_2.

Cell Compatibility: The L929 cells were used to assay the cell compatibility using the MTT test. The cells were incubated in a 96-well plate (8000 cells per well) and treated with fresh MEM culture medium in 5% CO_2 at 37 °C for 24 h. Then, $CeVO_4$ and $CeVO_4$/Ag at serial concentrations of 0, 12.5, 25, 50, 75, 100, 125, 150, 175, 200, 300, 400, 500, 600, 700 and 800 μg/mL were added to the above medium. Then, cells were incubated in 5% CO_2 at 37 °C for another 24 h. At the end of incubation, 10 μL of 3-[4, 5-dimethylthiazol-2-yl]-2, 5-diphenyltetrazolium bromide (MTT) solution was added into each well. The supernatant was aspirated after 4 h and 150 μL of dimethyl sulfoxide (DMSO) was added into each well. The viability of HeLa cells was evaluated using a microplate reader at 490 nm.

In vitro Cytotoxicity Evaluation: In vitro cytotoxicity of $CeVO_4$ and $CeVO_4$/Ag was assayed on HeLa cells by the MTT test. HeLa cells were incubated in a 96-well plate (8000 cells per well) and treated with fresh DMEM in 5% CO_2 at 37 °C for 24 h. Then, $CeVO_4$ and $CeVO_4$/Ag at serial concentrations of 0, 12.5, 25, 50, 75, 100, 125, 150, 175 and 200 μg/mL were added to the medium. After incubation for 4 h, the medium of HeLa cells was removed and the cells were washed once with PBS, and then the Hela cells were irradiated for 5 min with 808 nm laser (1.9 W/cm^2) in the fresh culture medium. Then, they were incubated again at 37 °C with 5% CO_2 for 24 h. At the end of incubation, MTT solution was added to each well. The supernatant was aspirated after 4 h and DMSO was added into each well. The viability of HeLa cells was evaluated using a microplate reader at 490 nm. The MTT assay of $CeVO_4$ and $CeVO_4$/Ag at 200 μg/mL with different power density (0.7, 1.0, 1.3, 1.6 and 1.9 W/cm^2) was also performed under the same situation.

Cellular Uptake: Fluorescein isothiocyanate (FITC) was labeled to $CeVO_4$ (labeled as $CeVO_4$-FITC) as follows: 2 mL of $CeVO_4$ nanosheets dispersed in 2 mL of THF solution. Then, 0.2 g of HS-PEG_{1000}-NH_2 and 100 μL of photoinitiator DMPA (10 mg/mL) dissolved in THF were added into it. The mixture was irradiated with UV-light (1000 W, 365 nm wavelength) for 60 min in an ice bath under magnetic stirring. After completion of UV irradiation, the $CeVO_4$-PEG_{1000}-NH_2 was collected by centrifugation at 12000 rpm for 15 min, and washed three times with deionized water. The 20 mg of above $CeVO_4$-PEG_{1000}-NH_2 was dispersed in 20 mL ethanol, then 20 μL of FITC (2 mg/mL) dissolved in ethanol was added into it. The mixture was refluxed at 80°C for another 12 h in the dark. Then, the $CeVO_4$-FITC were separated by centrifugation at 12000 rpm for 15 min, and washed with ethanol and dialysis against water (cutoff molecular weight: 12,000 Da) for one day.

HeLa cells were seeded in 6-well plate at a density of 1×10^5 cells per well and cultured overnight. Then the medium was replaced with fresh culture medium containing $CeVO_4$-FITC (200 μg/mL). After incubation for 4 h, the cells were washed with PBS several times and fixed with 4% paraformaldehyde for 10 min. For nucleus labeling, the cells were incubated with DAPI solution for 10 min. Then the medium was removal and rinsed with PBS several times. The celluar uptake was examined using a fluorescence microscope.

Cell Apoptosis: For flow cytometry, Hela cells were seeded into 6-well plates at a density of 2×10^5 cells per well and cultured overnight, and then treated with (a) control; (b) 808 nm laser irradiation only; (c) $CeVO_4$ (200 μg/mL); (d) $CeVO_4$/Ag (200 μg/mL); (e) $CeVO_4$ (200 μg/mL) + 808 nm laser and (f) $CeVO_4$/Ag (200 μg/mL) + 808 nm laser. After NIR light irradiation (1.9 W/cm^2, 5 min), all Hela cells were incubated for 24 h in 5% CO_2 at 37 °C. To obtain a single cell suspension, the Hela cells were handled using trypsinization and cold PBS, in sequence. Then, the cells were stained by the annexin V-

FITC and PI staining kit. Next, the induction of apoptosis was determined by A FACS Calibur flow cytometer (BD Biosciences).

Animal Xenograft Model: Female Balb/c mice (six weeks old) were purchased from the Center for Experimental Animals, Jilin University (Changchun, China). All animal studies were conducted in accordance with the guidelines of the National Regulation of China for Care and Use of Laboratory Animals. The H22 tumor model was established by subcutaneous injection with H22 cells into the left axilla of healthy Balb/c mice. When the tumor volume reached an approximate volume of 100 mm^3, the *in vivo* studies were carried out.

In vivo Phototherapeutic Efficacy: H22 tumor-bearing Balb/c mice with an average tumor volume of 100 mm^3 were randomly assigned into six groups: (a) control (only injected with saline), (b) 808 nm laser irradiation alone, (c) $CeVO_4$ injection alone, (d) $CeVO_4$/Ag injection alone, (e) $CeVO_4$ injection + 808 nm laser irradiation (0.7 W/cm^2) for 5 min and (f) $CeVO_4$/Ag injection + 808 nm laser irradiation (0.7 W/cm^2) for 5 min. All the groups were intratumorally injected with the same volume of saline, $CeVO_4$ or $CeVO_4$/Ag (100 µL, 20 mg/kg) solution. The tumor sizes and weight of mice were measured every 2 days. Tumor volume = length×$width^2$/2, relative tumor volume was calculated as V/V_0 (V_0 was the corresponding tumor volume when the treatment was initiated). These mice were sacrificed at day 14 to harvest the major organs for histological analysis.

Toxicology Evaluation: Healthy Balb/c mice were intravenously injected with saline (control group) and $CeVO_4$/Ag NCs at a dose of 20 mg/kg (test group), respectively. The weight of each group was recorded every 2 days. After injection at different times (day 1, day 7 and day 14), mice were euthanized and then the blood was collected for biochemistry analysis. In addition, the major organs (heart, liver, spleen, lung and kidney) were harvested and dissected to make paraffin sections for

further haematoxylin and eosin (H&E) staining.

Histological Analysis: Major organs (heart, liver, spleen, lung and kidney) were harvested, fixed in 10% neutral buffered formalin, processed routinely into paraffin, sectioned into thin slices and stained with H&E for histological analysis.

Bio-distribution of $CeVO_4$/Ag in Mice: Healthy Balb/c mice were injected with $CeVO_4$/Ag (100 μL, 20 mg/kg) intravenously. Then the mice (n = 4) were euthanized at different points in time (1 h, 6 h, 12 h, 1 day, 3 days, and 7 days). The major organs (heart, liver, spleen, lung and kidney) and tumors were collected in a beaker to be weighed. Then all of the organs and tumors were treated with concentrated nitric acid and H_2O_2 (v/v = 1:2) on heating (70 °C) until the solutions became clear. The concentrations of Ce and Ag in the solutions were measured by ICP-MS, and the concentrations in each organ and tumor were calculated.

Excretion Trace of $CeVO_4$/Ag NCs: $CeVO_4$/Ag NCs (20 mg/kg) were intravenously injected into mice (n = 3). And mice were placed in a metabolism cage. The feces and urine were collected and weighted every 24 h, and the contents of Ce and Ag were detected by ICP-MS.

***In vitro* and *In vivo* Photothermal Imaging:** For *in vitro* imaging, the aqueous $CeVO_4$ and $CeVO_4$/Ag solution (4 mg/mL, 100 μL) were placed in 96-well plates and were exposed to the NIR laser (808 nm, 0.7 W/cm^2) for 5 min. Simultaneously, an infrared camera was used to measure the real-time temperature, and the change in temperature was recorded every 1 min. For in vivo photothermal imaging, H22 cells were subcutaneously inoculated into the left armpit of Balb/c mice. When the tumor size reached about 100 mm^3, 100 μL of saline, $CeVO_4$ and $CeVO_4$/Ag (20 mg/kg) were intratumorally injected into the tumors, respectively. After injection, the tumor was exposed to NIR laser (0.7 W/cm^2), and IR images were recorded using infrared camera.

***In vitro* and *In vivo* PA Imaging:** To measure the photoacoustic (PA) signal sensitivity of $CeVO_4$ and $CeVO_4$/Ag, a phantom filled with the different concentrations of 0.03, 0.06, 0.125, 0.25 and 0.5 mg/mL nanoparticles was measured using a real-time multispectral optoacoustic tomographic (MSOT) imaging system (inVision 128, iThera Medical GmbH, Neuherberg, Germany). The phantom was then suspended inside a water tank and imaged at the 680–980 nm laser. Finally, the PA signals were measured in regions of interest (ROIs) for each sample and the correlation between the PA signal and concentration response curve was calculated.

To perform in vivo PA imaging, $CeVO_4$ and $CeVO_4$/Ag NCs (100 µL, 20 mg/kg) were intratumorally injected into the tumor-bearing mouse. Mouse was anesthetized with 2% isofluorane throughout the experiments, and placed in a horizontal position in a holder surrounded by a thin polyethylene membrane to prevent direct contact with water and allowed acoustic coupling between mouse and transducer array. The light fibers and ultrasonic transducer array were in a fixed position for all data acquisitions, whereas the mouse can be translated through the imaging plane using a linear stage. The mouse was scanned before and after intratumorally injection of $CeVO_4$ and $CeVO_4$/Ag. Regions of interests (ROIs) were selected and the PA signal was analyzed using ViewMOST^{TM} software.

Results and Discussion

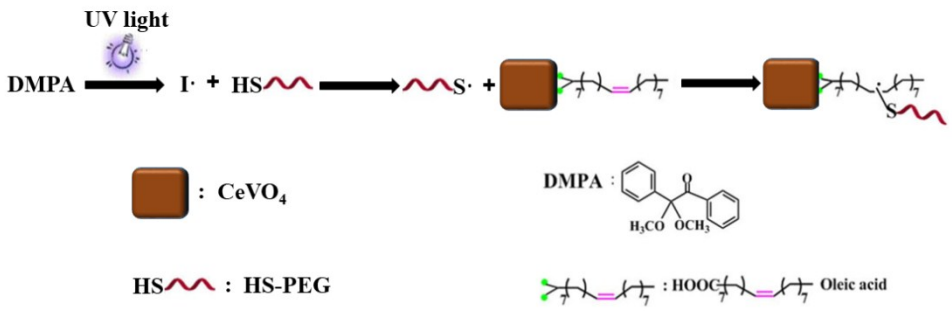

Fig. S1 Schematic illustration of the synthetic process for grafting HS-PEG on $CeVO_4$ NCs by thiol-ene click chemistry and the corresponding reactive mechanism.

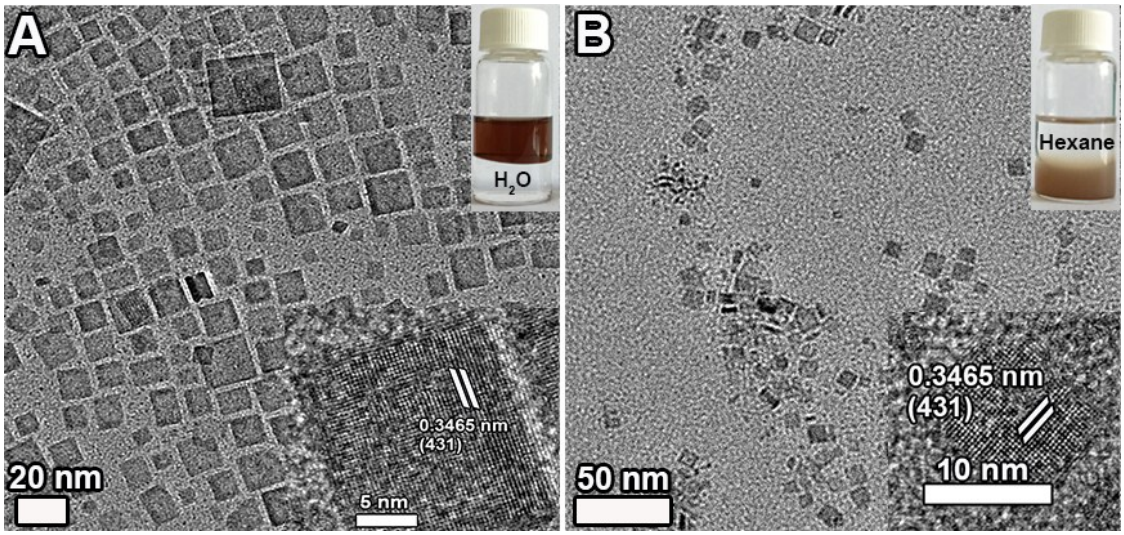

Fig. S2 TEM images of the OA-capped $CeVO_4$ dispersed in hexane (A) and $CeVO_4$ after modification with HS-PEG_{1000}-OH dispersed in THF (B). Digital photographs of OA-capped $CeVO_4$ dispersed in hexane and $CeVO_4$ modified by HS-PEG_{1000}-OH dispersed in water (inserts of A and B). HR-TEM image of OA-capped $CeVO_4$ (insert of A) and HR-TEM image of $CeVO_4$ modified by HS-PEG_{1000}-OH (insert of B).

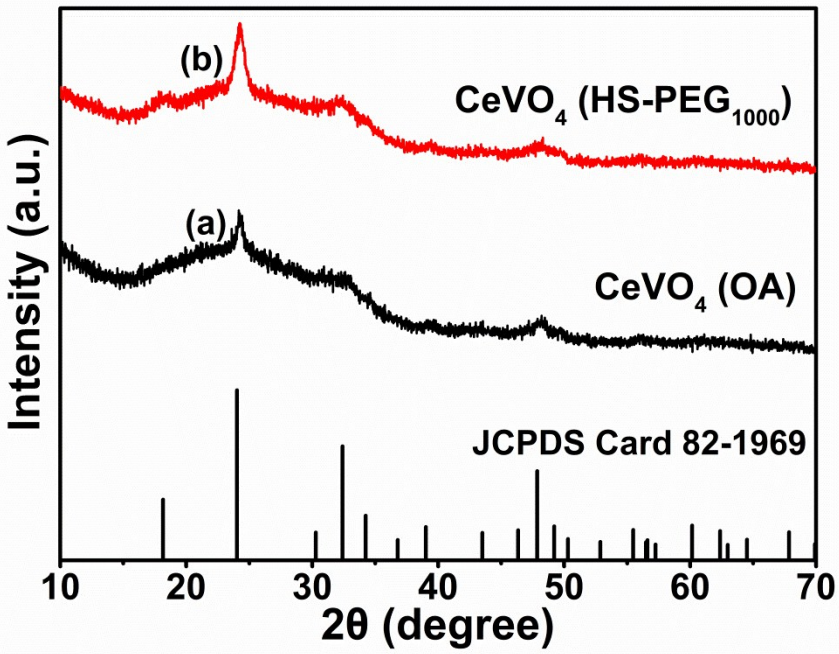

Fig. S3 XRD patterns of OA-capped $CeVO_4$ (a) and $CeVO_4$ after modification with HS-PEG_{1000}-OH (b).

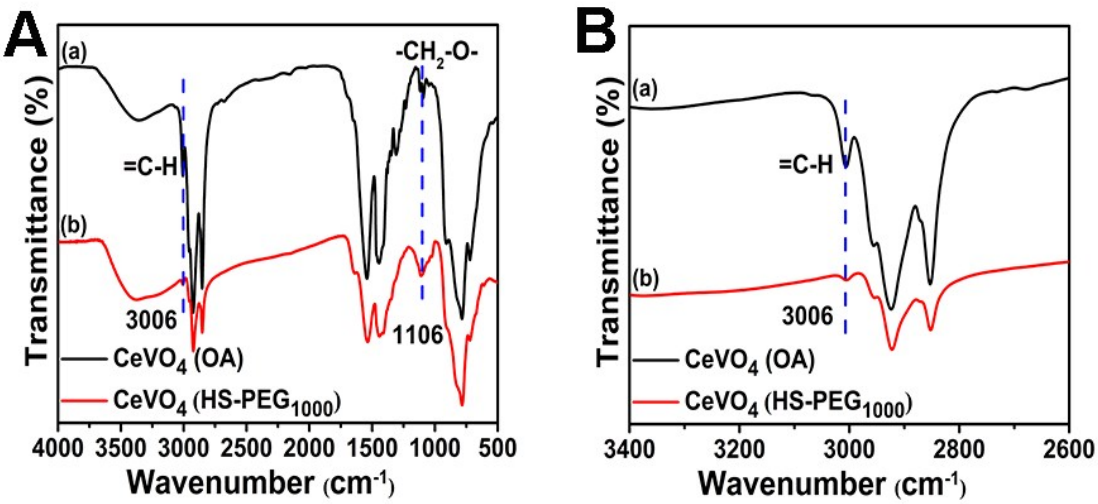

Fig. S4 (A) FTIR spectra of OA-capped $CeVO_4$ (a) and $CeVO_4$ modified by HS-PEG_{1000}-OH (b). (B) The enlarged region of Figure S3A for comparison.

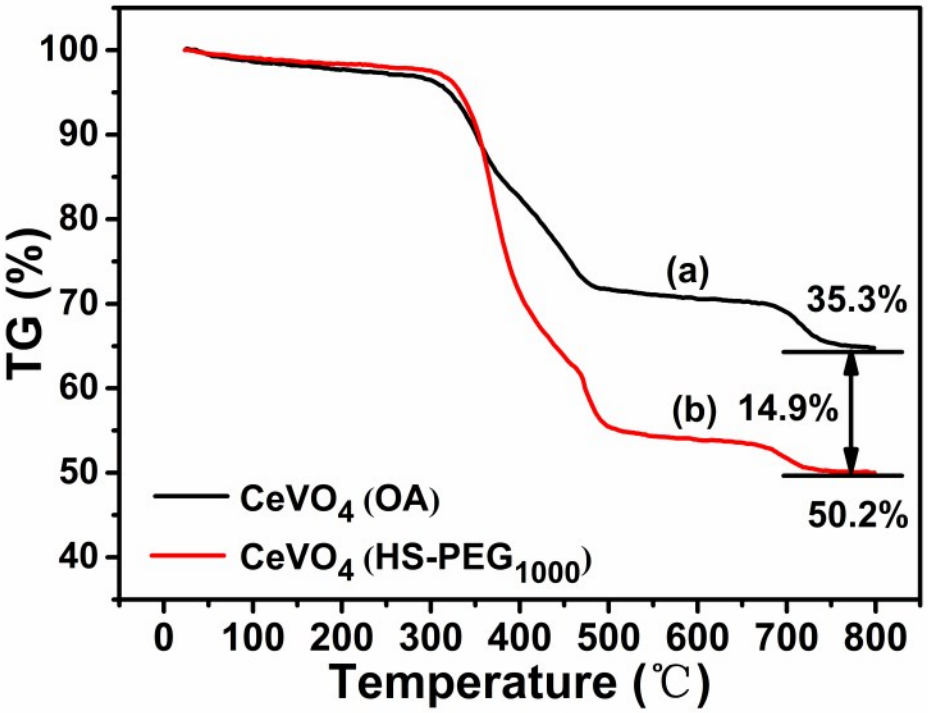

Fig. S5 TGA curves of $CeVO_4$ before (a) and after (b) modifying with HS-PEG_{1000}-OH.

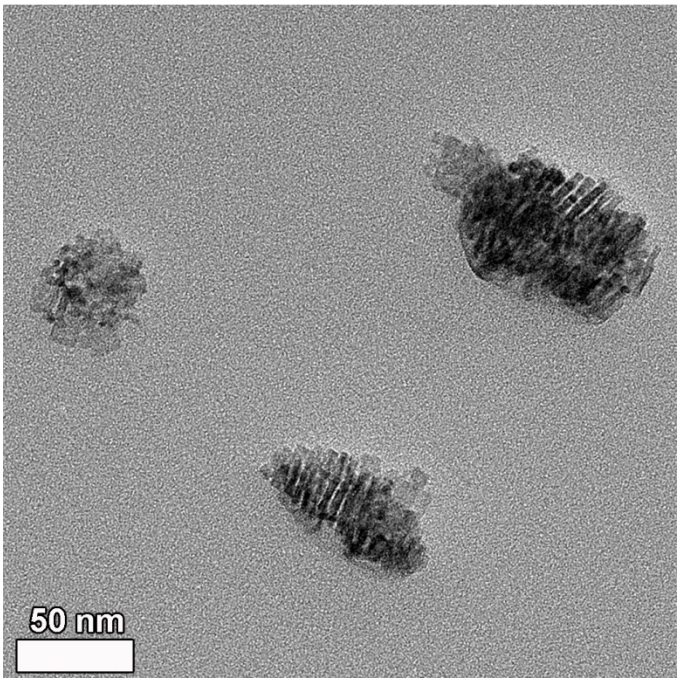

Fig. S6 TEM images of $CeVO_4$/Ag.

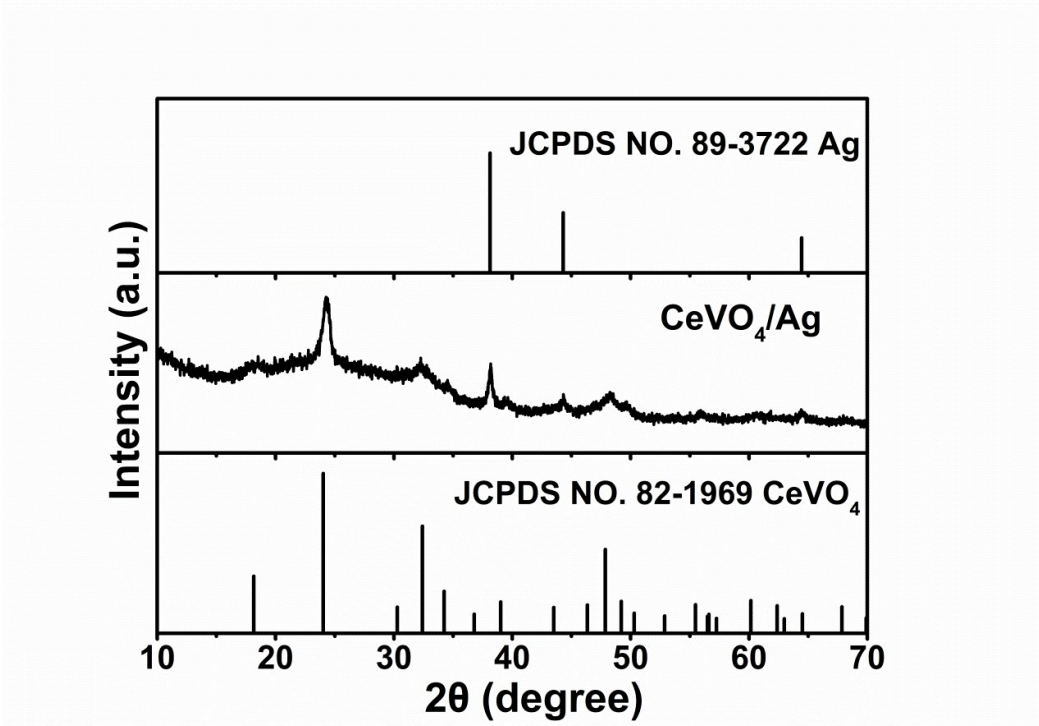

Fig. S7 XRD patterns of $CeVO_4$/Ag.

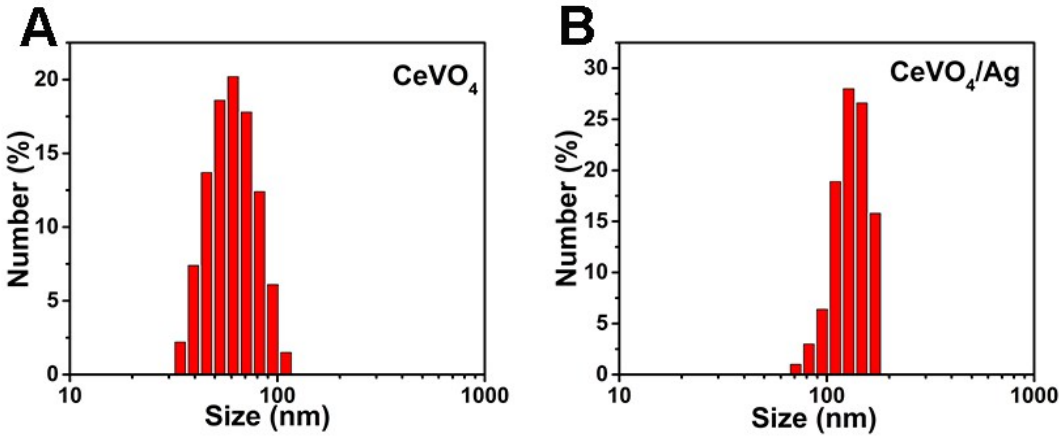

Fig. S8 Hydrodynamic size of $CeVO_4$ and $CeVO_4$/Ag.

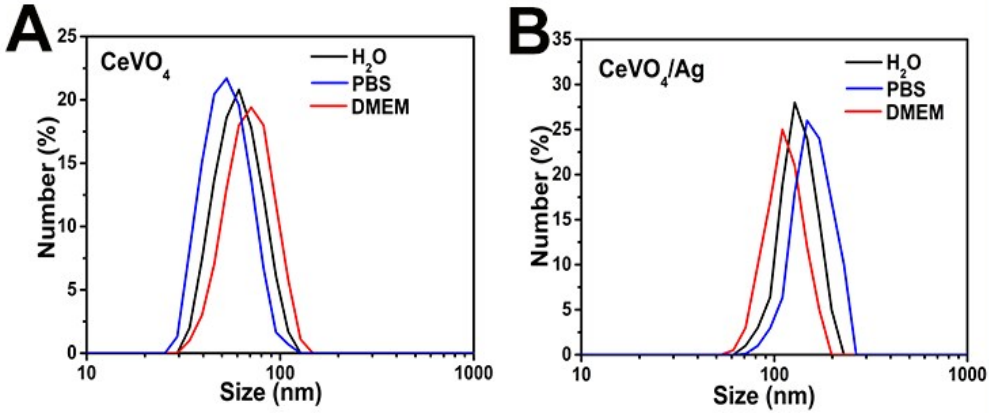

Fig. S9 The size distribution of $CeVO_4$ and $CeVO_4$/Ag measured in H_2O, PBS and DMEM containing 10% fetal bovine serum (FBS).

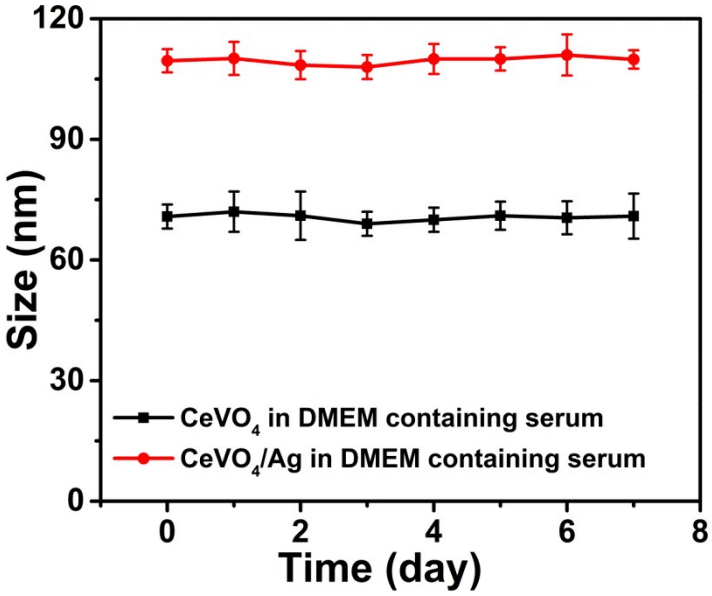

Fig. S10 The stability of $CeVO_4$ and $CeVO_4$/Ag in DMEM containing 10% FBS.

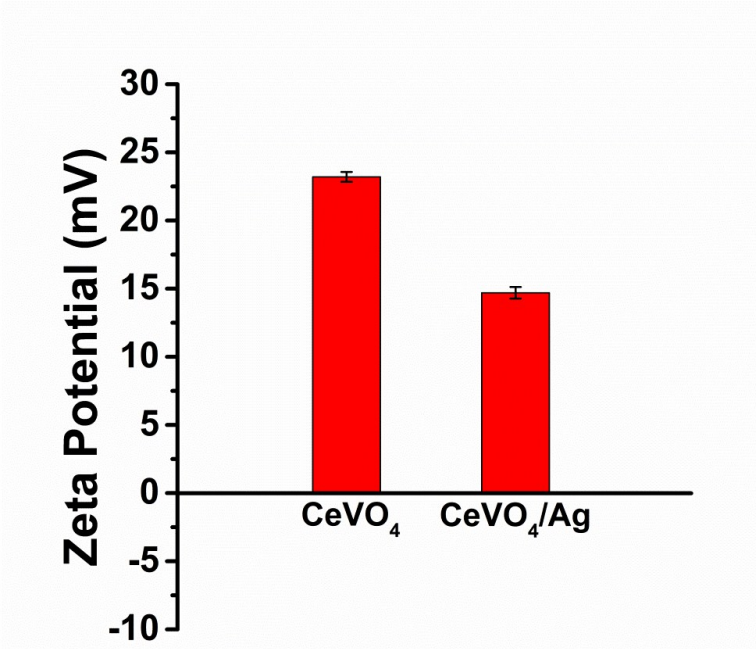

Fig. S11 The zeta potential of $CeVO_4$ and $CeVO_4$/Ag.

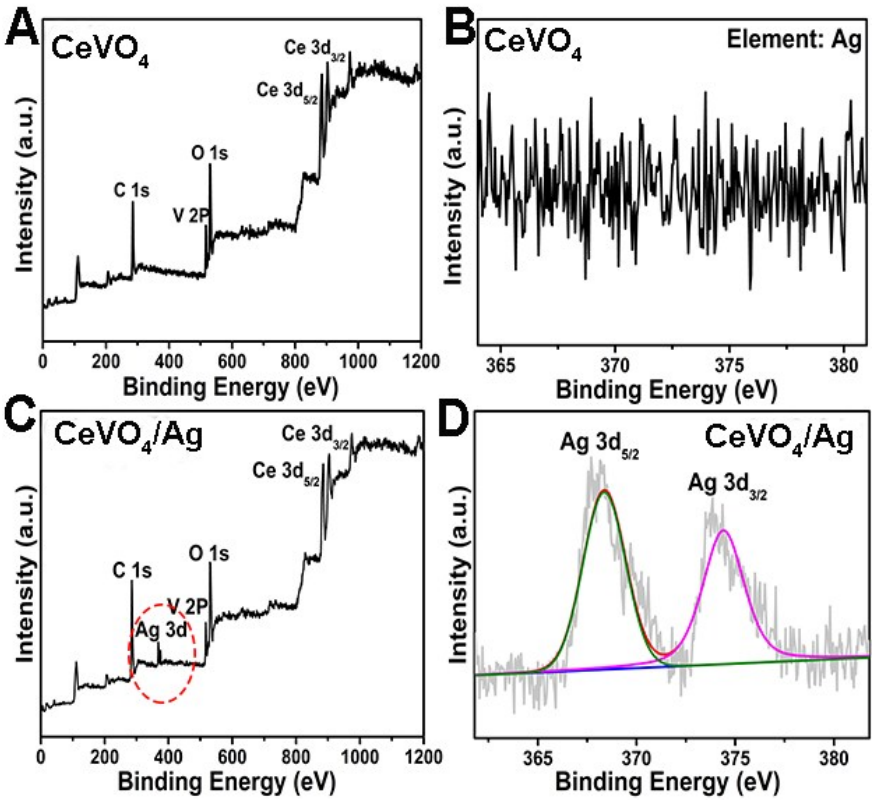

Fig. S12 XPS spectra of the $CeVO_4$ (A) and $CeVO_4$/Ag (C). XPS high-resolution scans of Ag 3d peaks in $CeVO_4$ (B) and $CeVO_4$/Ag (D).

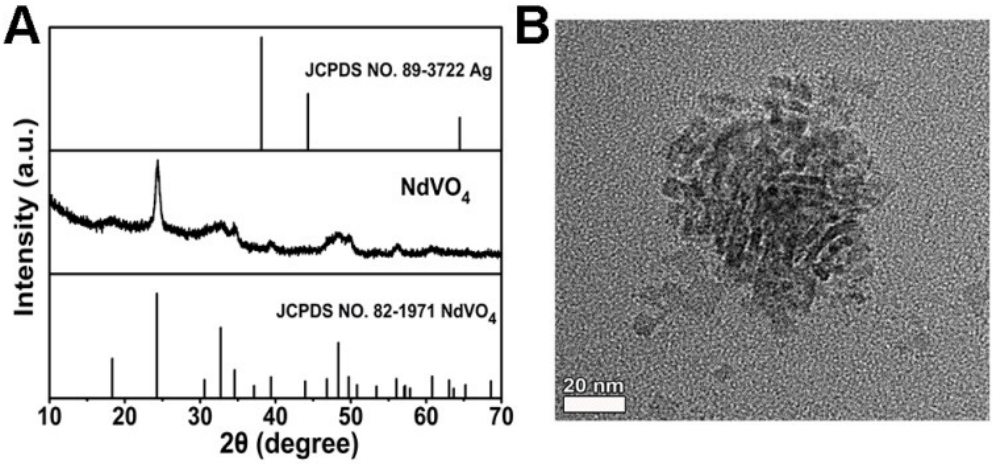

Fig. S13 The XRD patterns (A) and TEM images (B) of the ultimate product in control experiment.

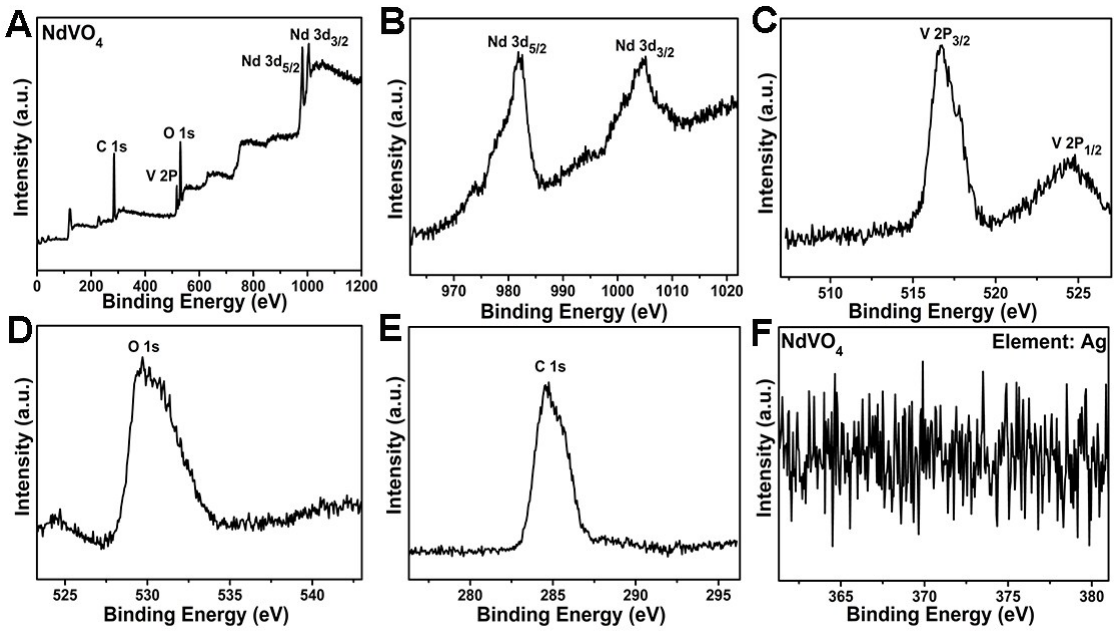

Fig. S14 (A) XPS spectra of the the ultimate product in control experiment. XPS high-resolution scans of Nd 3d (B), V 2p (C), O 1s (D), C 1s (E) and Ag 3d (F) peaks.

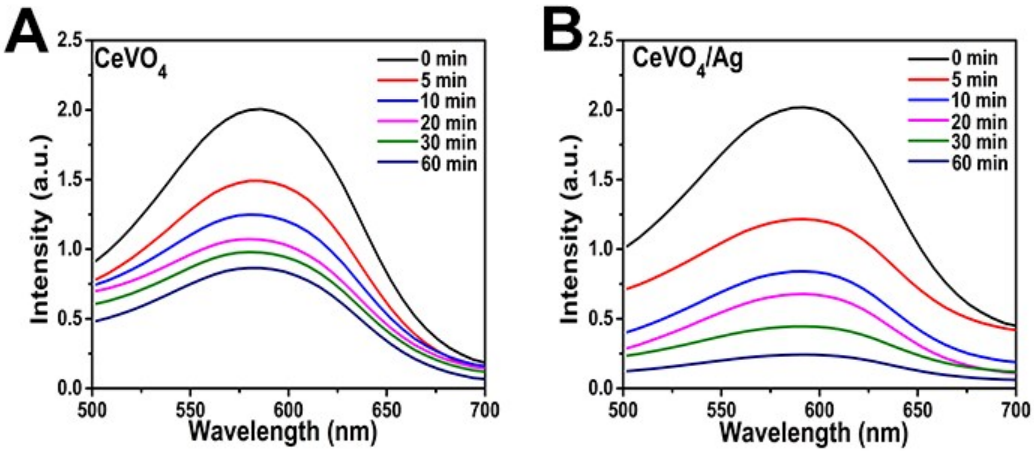

Fig. S15 Photocatalytic activity of $CeVO_4$ (A) and $CeVO_4$/Ag (B) under solar light.

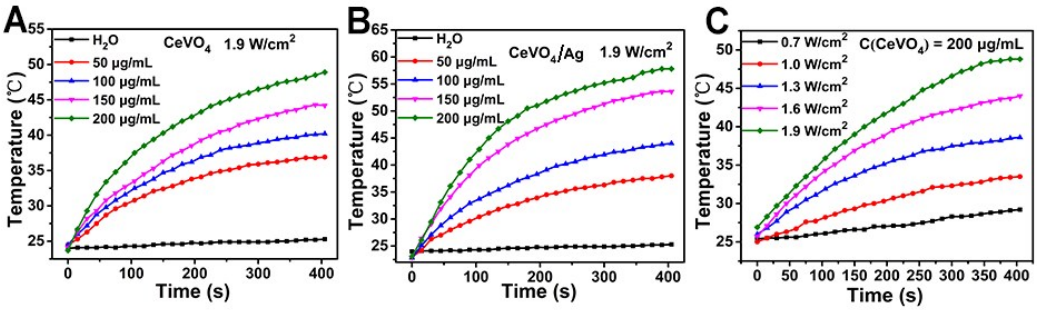

Fig. S16 Photothermal activity of $CeVO_4$ (A) and $CeVO_4$/Ag (B) with different concentration under 1.9 W/cm^2 808 nm laser irradiation for 5 min. (D) Photothermal activity of $CeVO_4$ with a concentration of 200 μg/mL under different power density of 808 nm laser irradiation for 5 min.

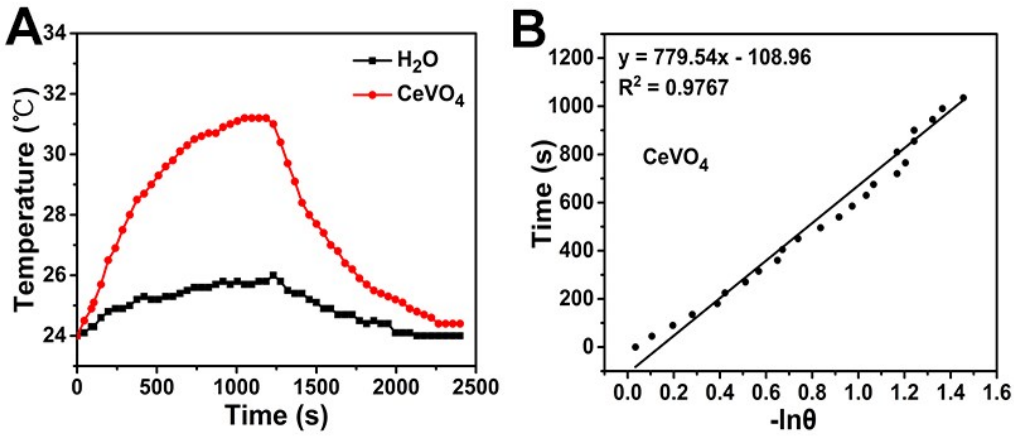

Fig. S17 (A) The temperature change of $CeVO_4$ aqueous solution (200 μg/mL, 1mL) and H_2O (1mL) response to 0.7 W/cm^2 808 nm laser on and off in period of 2400 s. (B) Linear time data versus -lnθ obtained from the cooling period of $CeVO_4$ aqueous solution.

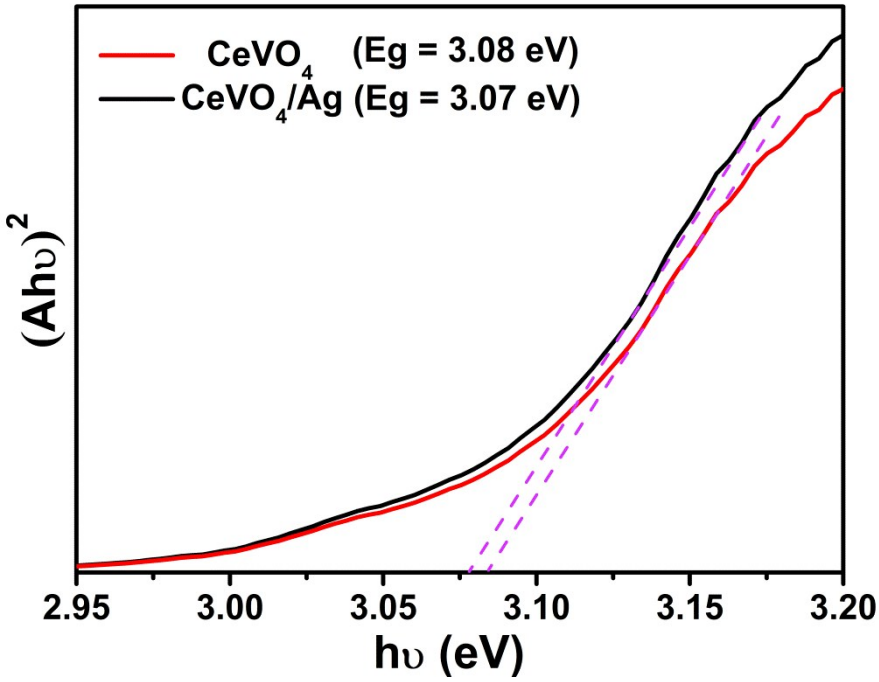

Fig. S18 Plots of $(Ah\upsilon)^2$ and photon energy (hυ) for the band gap energy of $CeVO_4$ and $CeVO_4$/Ag.

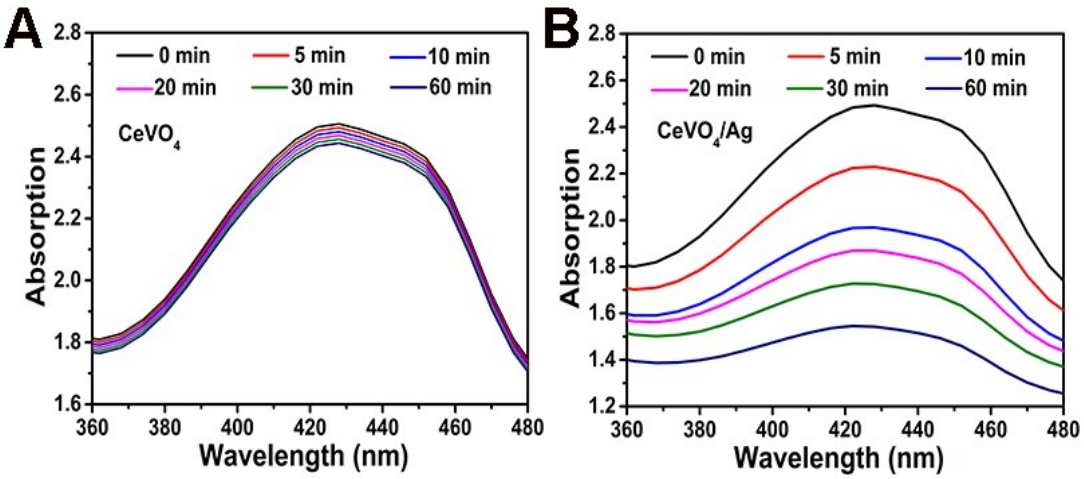

Fig. S19 Depletion of DPBF due to $\cdot O_2^-$ generation over $CeVO_4$ (A) and $CeVO_4$/Ag (B) with 808 nm laser irradiation.

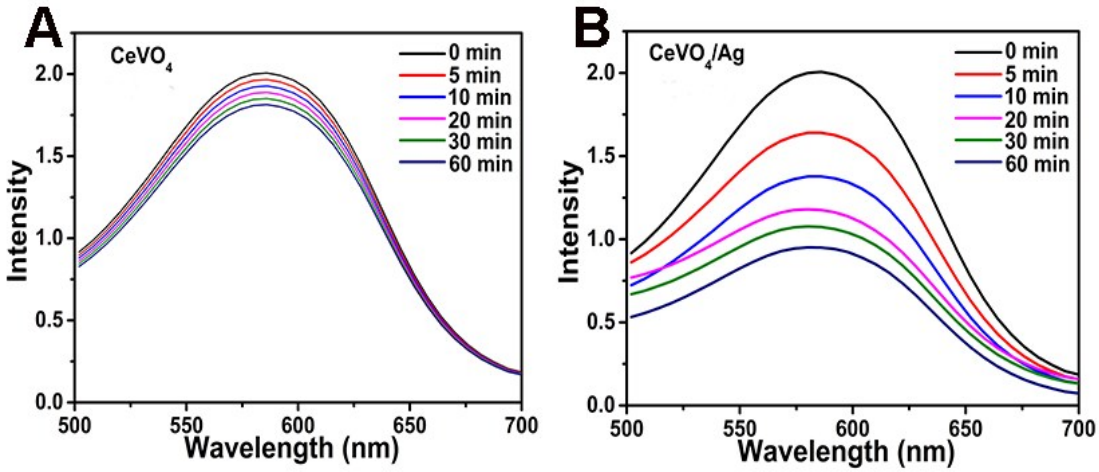

Fig. S20 Depletion of MB due to ·OH generation over $CeVO_4$ (A) and $CeVO_4$/Ag (B) with 808 nm laser irradiation.

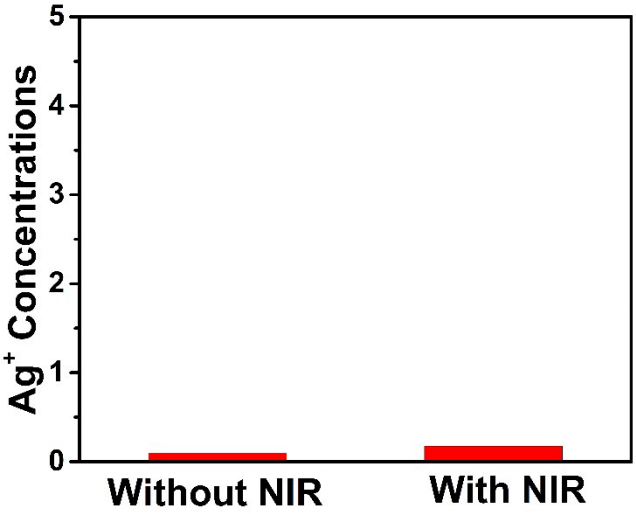

Fig. S21 Ag^+ release profiles from $CeVO_4$/Ag NCs.

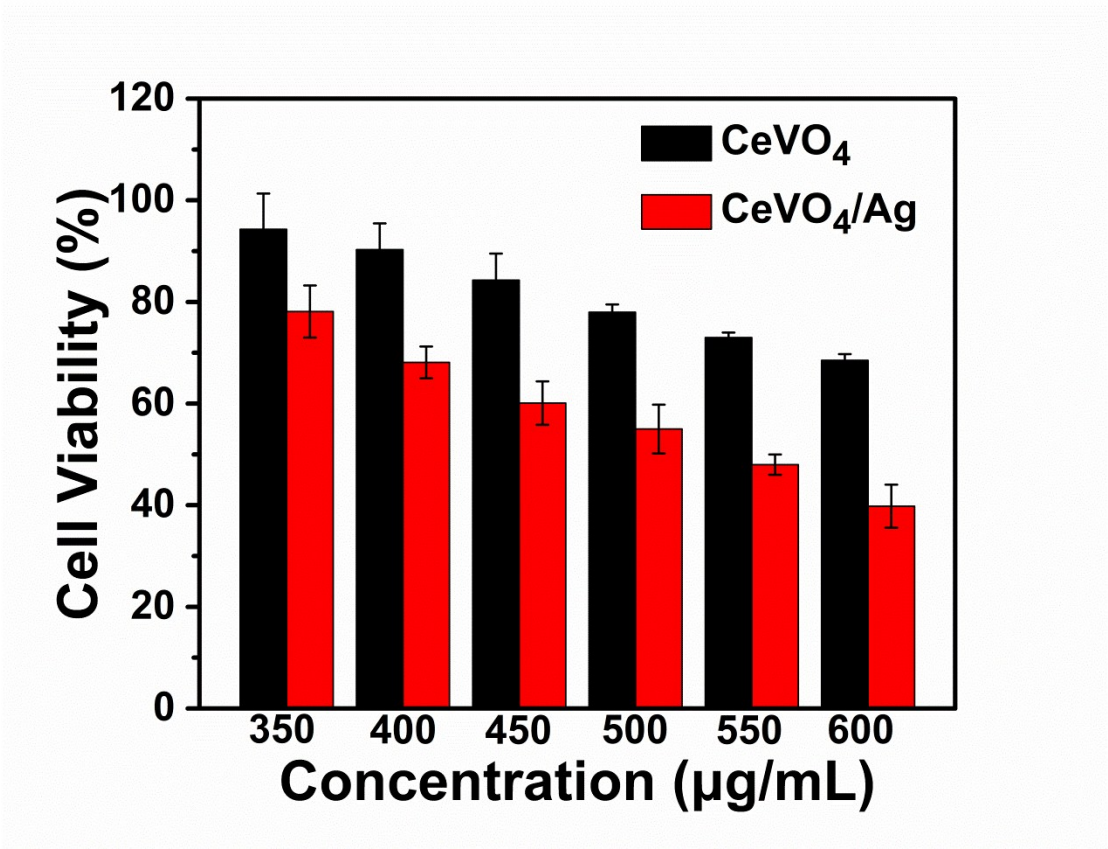

Fig. S22 L929 cells viability incubated with $CeVO_4$ and $CeVO_4$/Ag for 24h at different concentrations.

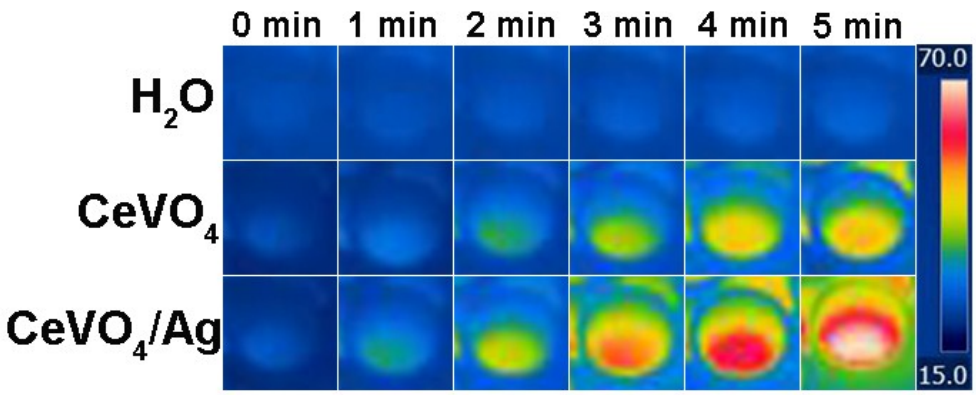

Fig. S23 The thermal images of H_2O, $CeVO_4$ and $CeVO_4$/Ag (4 mg/mL, 100 μL) exposed to 808 nm laser light (0.7 W/cm^2) for different times (0, 1, 2, 3, 4 and 5 min).

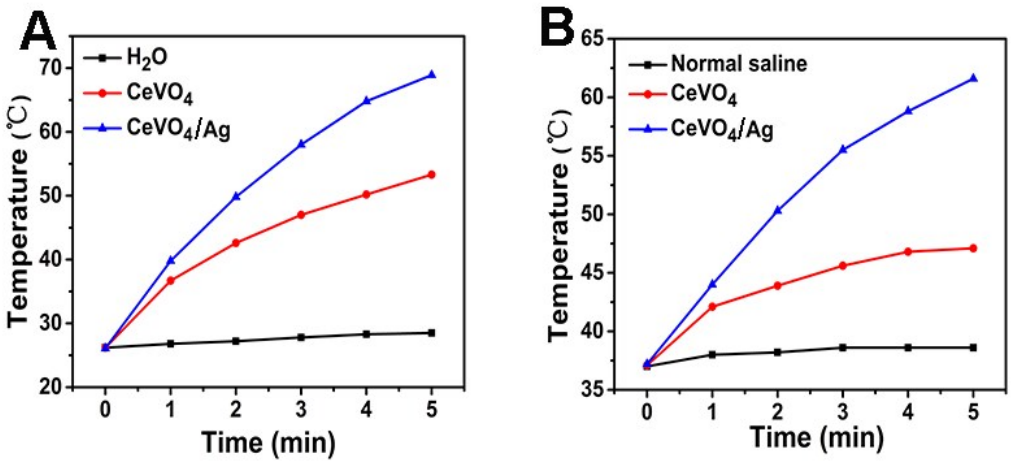

Fig. S24 (A) Temperature increasing curve of the *in vitro* thermal imaging of aqueous $CeVO_4$ and $CeVO_4$/Ag solution (4 mg/mL, 100 μL) and H_2O exposed to 808 nm laser light (1.3 W/cm^2) over time. (B) Temperature increasing curve of the H22-tumor-bearing mice with intratumor injection of normal saline, $CeVO_4$ and $CeVO_4$/Ag solution (20 mg/kg, 100 μL) exposed to 808 nm laser light (0.5 W/cm^2) over time.

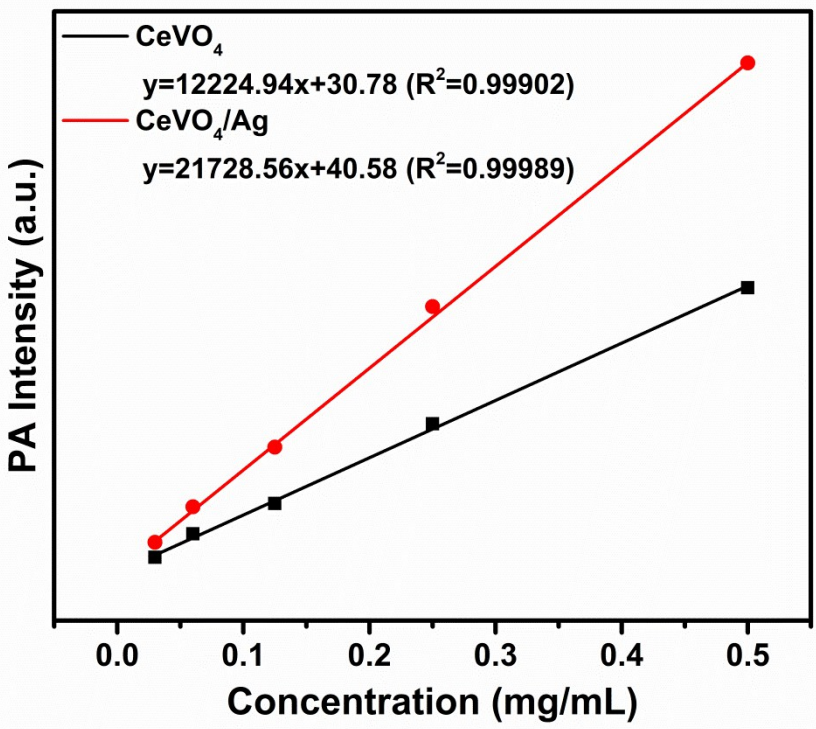

Fig. S25 Linear relationship between PA signal intensity and concentrations of $CeVO_4$ and $CeVO_4$/Ag, respectively.

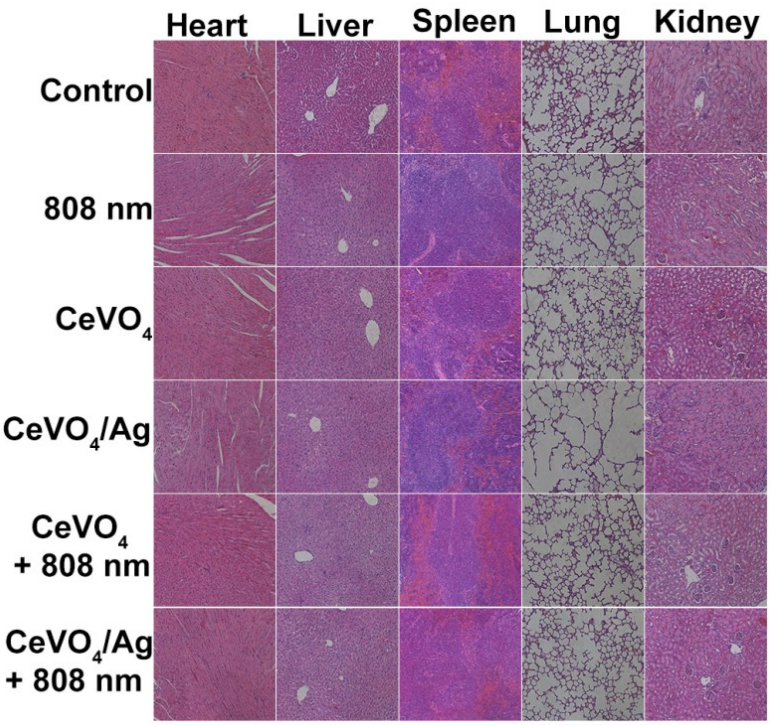

Fig. S26 The H&E stained images of major organs after the treatment with normal saline as control; 808 nm laser irradiation only; $CeVO_4$ only; $CeVO_4$/Ag only; $CeVO_4$ + 808 nm laser irradiation; $CeVO_4$/Ag + 808 nm laser irradiation (0.7 W/cm^2, 5 min).

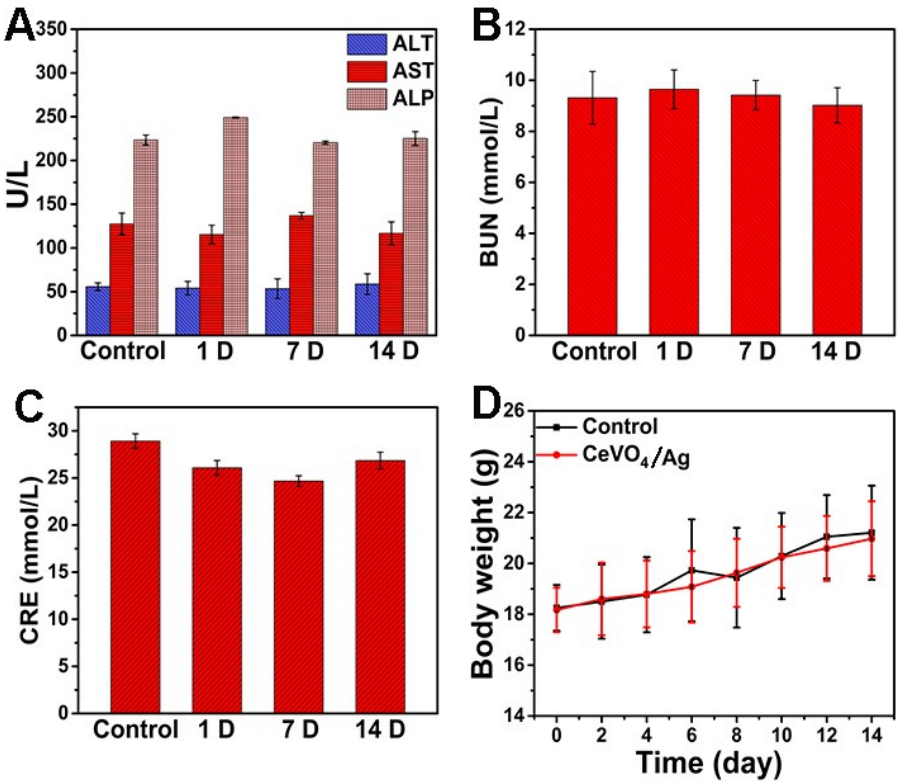

Fig. S27 (A-C) Blood serum biochemistry data of healthy Balb/c mice with intravenous injection of normal saline (control group) and $CeVO_4$/Ag (20 mg/kg, 100 μL). The data were collected at different time points of 1st, 7th, and 14th day. (D) Body weight change of Balb/c mice treated with $CeVO_4$/Ag (20 mg/kg, 100 μL) within 14 day compared to control group.

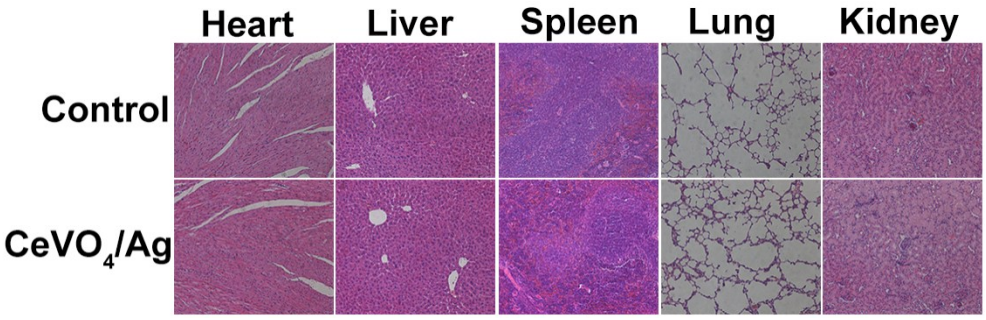

Fig. S28 The H&E stained histological slices from mice receiving intravenous injection of normal saline (control group) or $CeVO_4$/Ag (20 mg/kg, 100 μL) after 14 days.

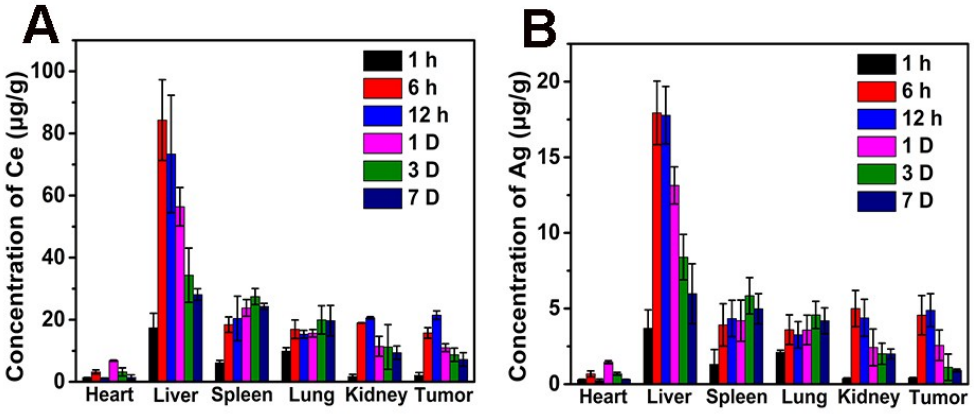

Fig. S29 Bio-distribution of Ce (A) and Ag (B) in major organs and tumors of mice after injection of $CeVO_4$/Ag (20 mg/kg, 100 μL) intravenously at different time points.

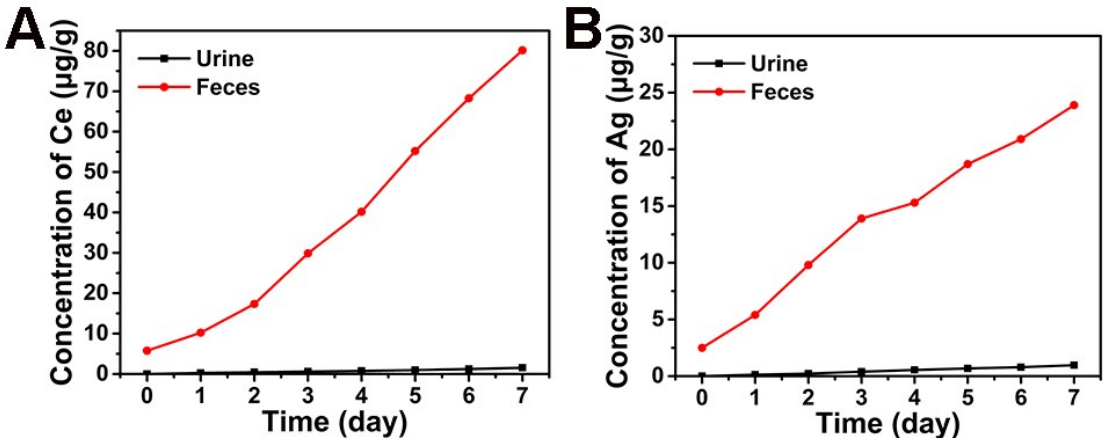

Fig. S30 The content of Ce (A) and Ag (B) in urine and feces collected at various time points after intravenous injection.

Table S1. The blood analysis parameters for control group and $CeVO_4$/Ag treated group, including alanine aminotransferase (ALT), alkaline phosphatase (ALP) and aspartate aminotransferase (AST) for hepatic function, blood urea (BUN) and serum creatinine (CRE) for renal function.

	Reference range	Untreated control	1 day	7 day	14 day
ALT (IU)	105 ± 65	55.75 ± 4.45	54.15 ± 7.75	53.55 ± 11.20	58.81 ± 11.75
AST (IU)	217 ± 150	127.51 ± 12.38	115.32 ± 10.81	136.91 ± 3.77	116.72 ± 13.12
ALP (IU)	187 ± 78	223.43 ± 5.76	249.04 ± 0.75	220.39 ± 1.68	225.18 ± 7.93
BUN (mmol/L)	20 ± 13	9.32 ± 1.03	9.65 ± 0.76	9.42 ± 0.57	9.03 ± 0.69
CRE (mmol/L)	35 ± 15	28.92 ± 0.78	26.08 ± 0.78	24.67 ± 0.57	26.85 ± 0.89

References

1 J. Liu and Y. Li, *J. Mater. Chem.*, 2007, **17**, 1797.
2 B. Liu, X. Deng, Z. Xie, Z. Cheng, P. Yang and J. Lin, *Adv. Mater.*, 2017, **29**.